Available online at www.sciencedirect.com
ScienceDirect
Trans. Nonferrous Met. Soc. China 23(2013) 2560−2567
Transactions of Nonferrous Metals Society of China
www.tnmsc.cn

Hot compression behavior and deformation microstructure of Mg−6Zn−1Al−0.3Mn magnesium alloy

Bao-liang SHI, Tian-jiao LUO, Jing WANG, Yuan-sheng YANG

Institute of Metal Research, Chinese Academy of Sciences, Shenyang 110016, China

Received 21 July 2012; accepted 25 June 2013

Abstract: The hot compression behavior of a wrought Mg−6Zn−1Al−0.3Mn magnesium alloy was investigated using Gleeble test at 200−400 °C with strain rates ranging from 0.01 to 7 s^{-1}. The true stress—strain curves show that the hot deformation behavior significantly depends on the deformation temperature and strain rate. The calculated hot deformation activation energy Q is 166 kJ/mol with a stress exponent n=5.99, and the constitutive equation is deduced to be $\dot{\varepsilon}=3.16\times10^{13}[\sinh(0.010\sigma)]^{5.99}\exp[-1.66\times10^5/(RT)]$· Deformation microstructure shows that the incompletely dynamically recrystallized grains can be found at grain boundaries and twins with the strain rates ranging from 0.01 to 1 s^{-1} at 250 °C, and completely dynamic recrystallization occurs when the temperature is 350 °C or above during hot compression, the size of recrystallized grains decreases with the increment of the strain rate at the same temperature. The relatively suitable deformation condition is considered temperature 330−400 °C and strain rate of 0.01−0.03 s^{-1}, and temperature of 350 °C and strain rate of 1 s^{-1}.

Key words: wrought magnesium alloy; hot compression; stress; strain; recrystallization

1 Introduction

Wrought magnesium alloys have great potentials due to their higher strength and ductility, such as Mg−Al−Zn (AZ31, AZ61, AZ80) alloys, which have been widely used in automobile, electronic and communication industries [1−3]. Mg−Al−Zn alloys have a poor creep resistance due to the discontinuous precipitation and coarsening of $Mg_{17}Al_{12}$, and the $Mg_{17}Al_{12}$ phase is prone to break, resulting in the decrease of strength and ductility [4,5]. Compared with Mg−Al−Zn alloys, Mg−Zn alloys have higher mechanical properties at ambient and elevated temperatures because of the significant age hardening response and stable Mg−Zn phase precipitations in the alloys. For example, ZK60 is the typical high strength wrought magnesium alloy [6−8]. However, Zr addition to Mg−Zn series alloys increases the costs and difficulties in melting [9], so development of low cost wrought magnesium with high strength is an important trend. Mg−6Zn magnesium alloy with Al addition has been proved to contribute to double aging after solution heat treatment and morphology change and distribution of the precipitates, which enhances the alloy strength [10,11]. Therefore, Mg−Zn−Al magnesium alloy may be a new potential wrought magnesium with low cost and high strength. However, there is a lack of study on the hot deformation of Mg−6Zn−1Al magnesium alloy.

In the present study, the hot deformation behavior of cast Mg−6Zn−1Al−0.3Mn magnesium alloy was investigated by compression test at temperature between 200 and 400 °C and strain rates ranging from 0.01 to 7 s^{-1}. The constitutive equation was calculated, and the deformation microstructure was analyzed. In addition, the suitable deformation condition was concluded based on the analysis of compression behavior and deformation microstructure by the processing maps.

2 Experimental

Ingots with a nominal composition of Mg−6Zn−1Al−0.3Mn (mass fraction, %) alloy (ZA61) were cast, and the cylindrical specimens (d8 mm×12 mm) for the compression tests were cut from the ingots which were subjected to homogenization treatment at 400 °C

Foundation item: Project (2011BAE22B01-1) supported by the National Key Technologies R&D Program of China; Project (2011DFA50903) supported by the International S&T Cooperation Program of China
Corresponding author: Yuan-sheng YANG; Tel: +86-24-23971728; Fax: +86-24-23844528; E-mail: ysyang@imr.ac.cn
DOI: 10.1016/S1003-6326(13)62768-5

for 12 h. Hot compression tests were carried out at strain rates of 0.01, 0.1, 1, 3, 5, 7 s^{-1} and deformation temperatures of 200, 250, 300, 350, 400 °C with Gleeble 3800 machine servo-controlled by a computer. The specimens for compression test were pre-heated up to the deformation temperature at a heating rate of 5 °C /s and held for 5 min before compression test. All the specimens were compressed to 60% true strain or to be broken. After compression test, the specimens were water quenched immediately to keep the deformation microstructure to room temperature. The samples were cut from the deformed specimens along the deformation direction at the middle. The samples were observed using a MM-6 metallographic microscope after being etched with a solution of 1.5 g picric acid, 5 mL acetic acid, 10 mL distilled water and 25 mL ethanol.

3 Results and discussion

3.1 True stress—strain curves

Typical true stress—true strain curves during hot compression of the test ZA61 alloy at various strain rates and temperatures are presented in Fig. 1. It is shown that the flow stress first increases with strain up to peak stress, and then decreases to a relatively steady value, which is a typical characteristic of hot working accompanied by dynamic softening [12]. Besides, the strain rate and deformation temperature have an important influence on the flow stress. When deformed at the same strain rate, the flow stress decreases with the increase of temperature, and the flow stress increases with the increase of the strain rate at a fixed temperature.

Figure 2 shows the peak stress as a function of temperature at different strain rates. It is clear that the peak stress depends on the temperature and strain rate, and the stress increases with increasing the strain rate at a certain temperature. On the other hand, the peak stress decreases with increasing the temperature at a given strain rate. This is because the increase of strain rate will produce a higher dislocation density every time, which causes stronger work-hardening. At the same time, the increased strain rate weakens dynamic softening effect. At a given strain rate, the critical resolved shear stress for non-basal slip declines with increasing temperature and non-basal dislocations are easily activated. Besides, both the softening effects of dynamic recovery and dynamic recrystallization get strengthened, which results in the decrease of flow stress. It should be pointed out that the slope of the linear dependence decreases more sharply below 300 °C compared with that under higher

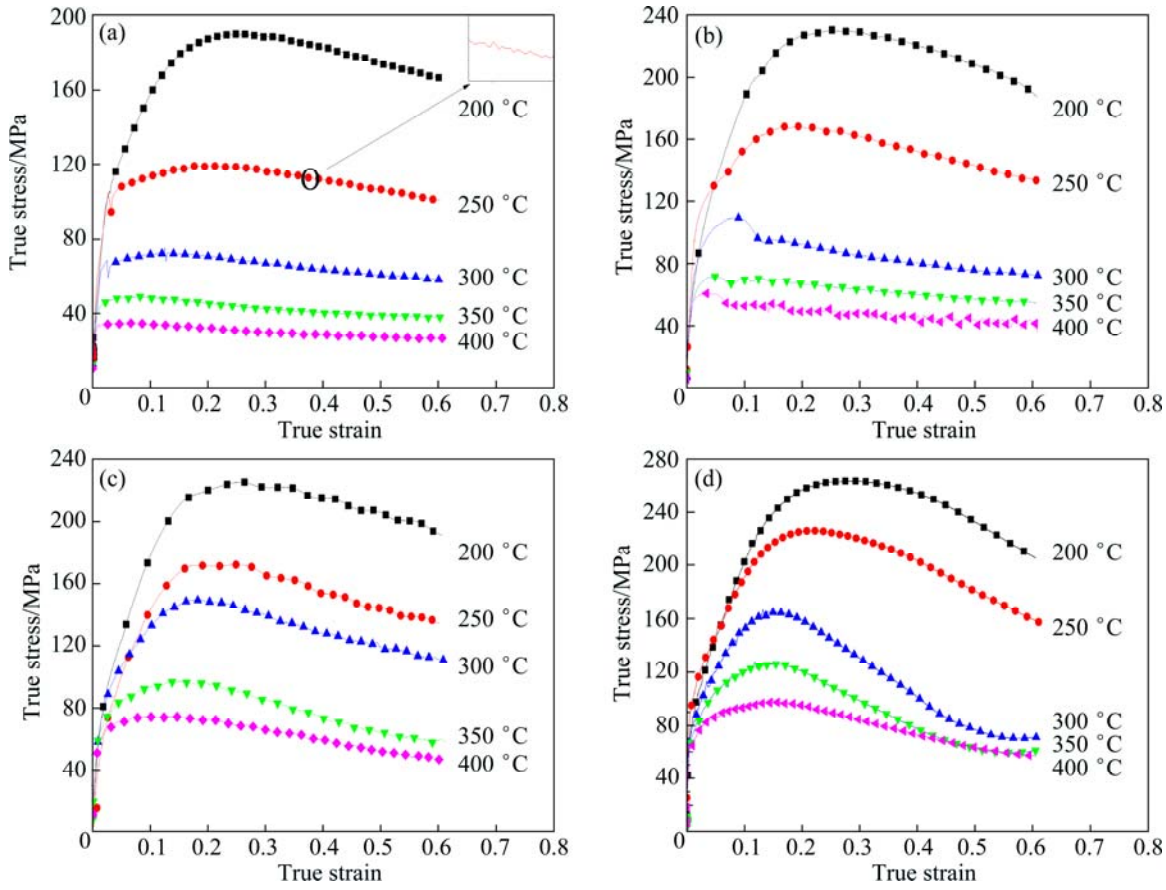

Fig. 1 Typical true stress—strain curves of experimental alloy obtained by hot compression tests at different strain rates: (a) 0.01 s^{-1}; (b) 0.1 s^{-1}; (c) 1 s^{-1}; (d) 7 s^{-1}

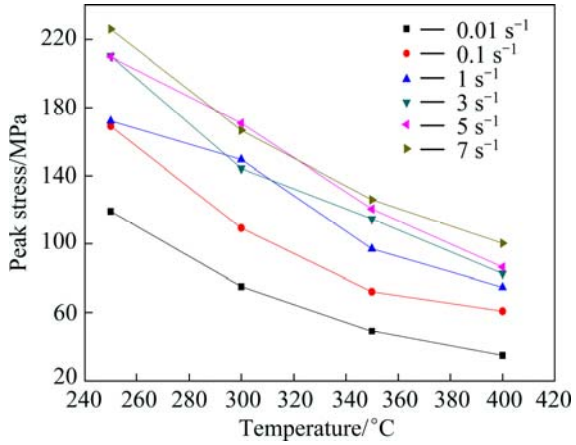

Fig. 2 Dependence of peak stress on temperature at given strain rates

temperatures, which suggests that the increase of temperature below 300 °C has a better softening influence on the flow stress. Thus, the processing temperature of the ZA61 magnesium alloy should be higher than 300 °C due to the lower flow stress.

3.2 Constitutive analysis

The effects of strain rate and temperature on hot deformation behaviors can be expressed by the hyperbolic sine-type equation [13,14] over a wide range of stress:

$$\dot{\varepsilon} = A[\sinh(\alpha\sigma)]^n \exp[-Q/(RT)] \quad (1)$$

where $\dot{\varepsilon}$ is the strain rate; Q is the activation energy of deformation; R is the gas constant of 8.314 J/K; T is the deformation temperature; A, α and n are the material constants independent of σ and T.

To simplify the equation, taking the natural logarithms of both sides of the equation, then we get

$$\ln\dot{\varepsilon} = \ln A - Q/(RT) + n\ln[\sinh(\alpha\sigma)] \quad (2)$$

Based on Eq. (2), the activation energy can be expressed as

$$Q = Rnb = R\left(\frac{\partial\ln\dot{\varepsilon}}{\partial\ln[\sinh(\alpha\sigma)]}\right)_T\left(\frac{\partial\ln[\sinh(\alpha\sigma)]}{\partial 1/T}\right)_{\dot{\varepsilon}} \quad (3)$$

where n and b are the average slope values of the plots of $\ln\dot{\varepsilon}$ — $\ln[\sinh(\alpha\sigma)]$ at constant temperatures and $\ln[\sinh(\alpha\sigma)]$—$1/T$ at constant strain rates, respectively. Meantime, the optimum value of α can be obtained, when the curves in the $\ln[\sinh(\alpha\sigma)]$ against $\ln\dot{\varepsilon}$ at constant temperature are almost linear and parallel to each other, and α was 0.010 in the present work.

The variation of $\ln\dot{\varepsilon}$ — $\ln[\sinh(\alpha\sigma)]$ at different temperatures is shown in Fig. 3. The average value of the stress exponent n was calculated as 5.99, with a maximum deviation of approximately 2.3%. The n usually relates to the deformation mechanism of metals. It is verified that climb-controlled dislocation creep is the dominant deformation process for the n ranging from 5 to 7 [15,16]. So, it could be thought that the hot deformation mechanism of the tested ZA61 is climb-controlled dislocation creep, which indicates that the metal exhibits moderate ductility at elevated temperatures. It is expected that the plastic forming behaviors for the ZA61 Mg alloy, such as deep drawing and forging may be possible to be performed under the deformation conditions.

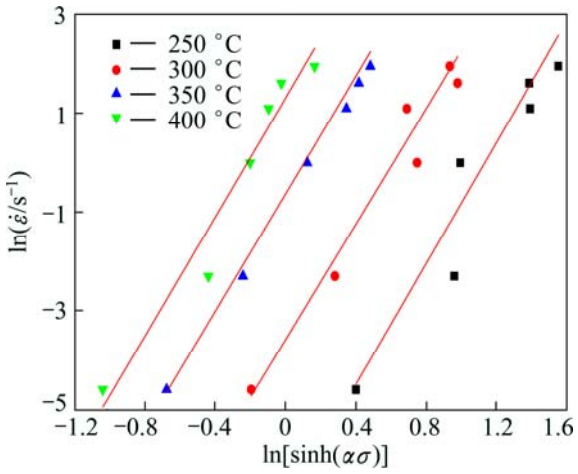

Fig. 3 Variation of $\ln\dot{\varepsilon}$ vs $\ln[\sinh(\alpha\sigma)]$ at different temperatures

Figure 4 shows the variation of $\ln[\sinh(\alpha\sigma)]$—$1/T$ at different strain rates. The average linear dependent coefficients reach 0.98, and the average activation energy derived from above calculations is 166 kJ/mol in the present experiment. So, when substituting Q, A, n into Eq. (1), the constitutive equation of the ZA61 Mg alloy can be expressed as

$$\dot{\varepsilon} = 3.16\times10^{13}\left[\sinh(0.010\sigma)\right]^{5.99}\exp[-1.66\times10^5/(RT)]$$

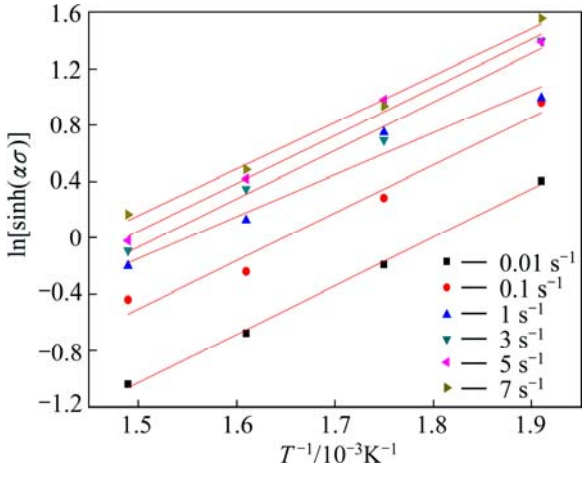

Fig. 4 Variation of $\ln[\sinh(\alpha\sigma)]$—$1/T$ at different strain rates

3.3 Deformation microstructure and recrystallization

The effect of temperature on the deformed microstructures of the hot compressed ZA61 Mg alloy at the strain rate of 0.01 s^{-1} is shown in Fig. 5. The microstructure deformed at 200 °C shows no apparent dynamic recrystallization. When the deformation temperature reaches 250 °C, fine dynamically recrystallized grains occur around the initial grains elongated along the direction perpendicular to the compression direction, which is typical of 'necklace' type dynamic recrystallization. Meanwhile, both the volume fraction and the size of the dynamically recrystallized grains are increased with increasing temperature. It is clear that the microstructure is completely dynamically recrystallized at 350 °C or above, and the size of grains is largely refined compared with the initial microstructure.

Figure 6 shows the microstructures of hot deformed ZA61 magnesium alloy at 250 °C with different strain rates. It is evident that fine and incomplete dynamically recrystallized grains can be found at grain boundaries and twins with the strain rates ranging from 0.01 to 1 s^{-1} at 250 °C. However, there are nearly no initialized recrystallized grains when the strain rate reaches 7 s^{-1}. On one hand, magnesium and magnesium alloys have a low stacking fault energy, and the stacking fault energy of pure magnesium is only 60−78 mJ/m^2 [9], the width of extended dislocation is large, hence dynamically recovery is difficult to occur due to the restriction of cross-slip and the climb of edge dislocation, which contributes to the dynamical recrystallization at the initial grain boundary. On the other hand, the recrystallized grains can be induced by twinning [17], so fine recrystallized grains could be observed at grain boundaries and twins at 250 °C. However, the low deformation temperature cannot provide enough energy for the movement of dislocations, and twins are more stable than dislocations at low temperatures, both of

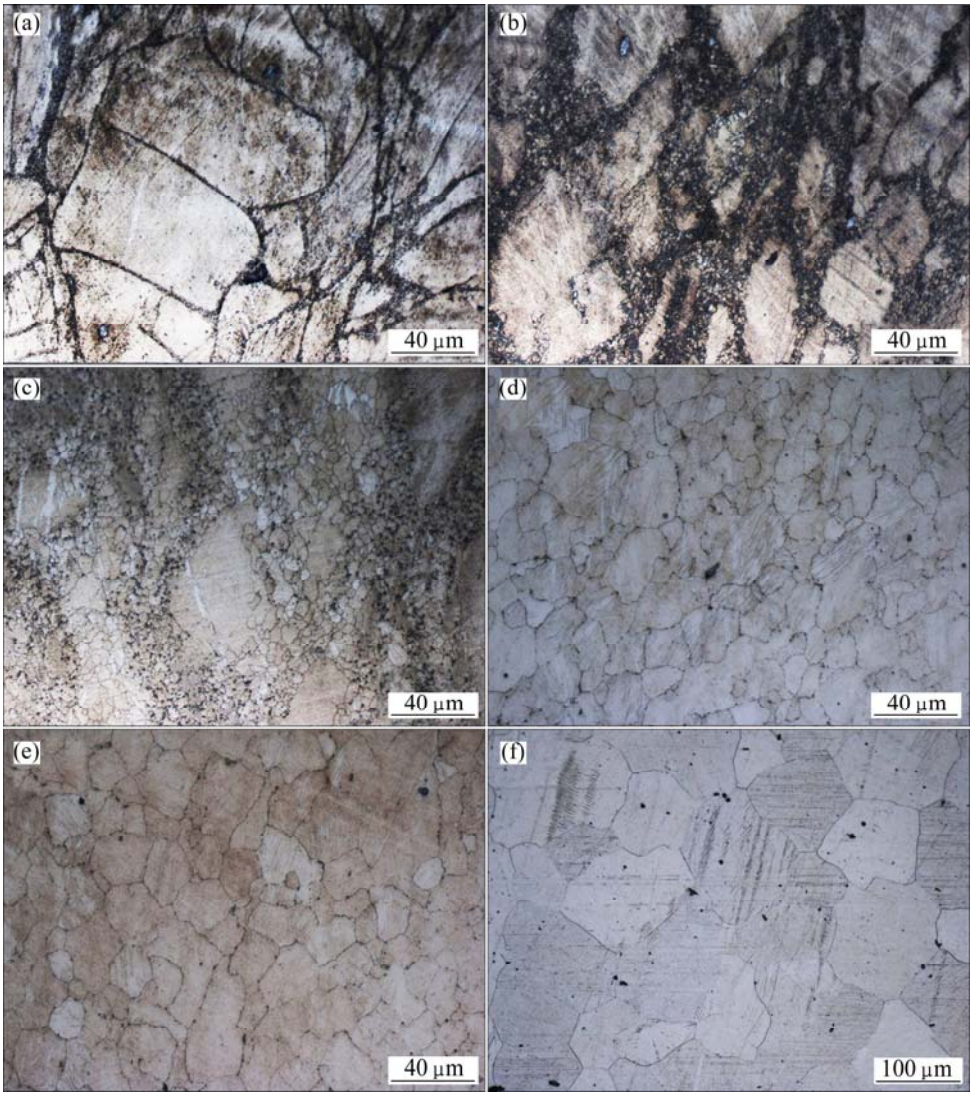

Fig. 5 Optical microstructures of hot compressed ZA61 Mg alloy with compression strain of 60% at strain rate of 0.01 s^{-1} and different temperatures: (a) 200 °C; (b) 250 °C; (c) 300 °C; (d) 350 °C; (e) 400 °C; (f) Before hot compression

which cause the incompletely dynamic recrystallization, and little dynamically recrystallized grains are presented at the strain rate of 7 s^{-1}.

Microstructures of the ZA61 Mg alloy with compression strain of 60% at 350 °C and 400 °C with different strain rates are presented in Fig. 7. It can be seen that completely dynamic recrystallization occurred at 350 °C and 400 °C with the strain rate of 0.01−1 s^{-1}, and fine recrystallized grains are developed homogeneously. The recrystallized grain size is reduced

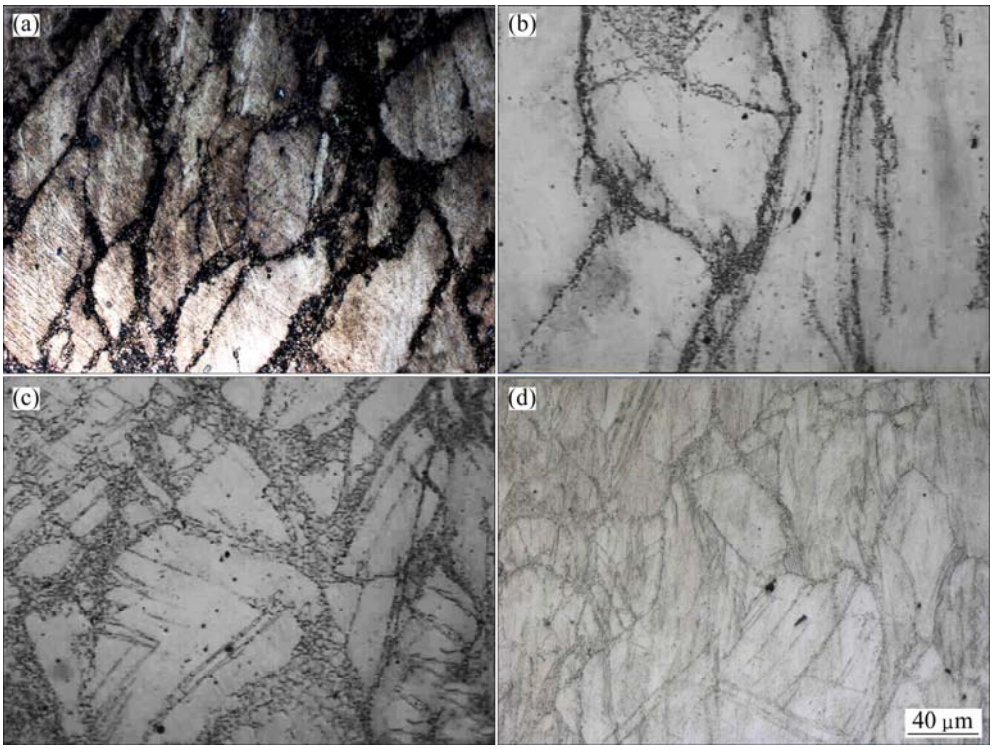

Fig. 6 Optical microstructures of ZA61 Mg alloy with compression strain of 60% at 250 °C under different strain rates: (a) 0.01 s^{-1}; (b) 0.1 s^{-1}; (c) 1 s^{-1}; (d) 7 s^{-1}

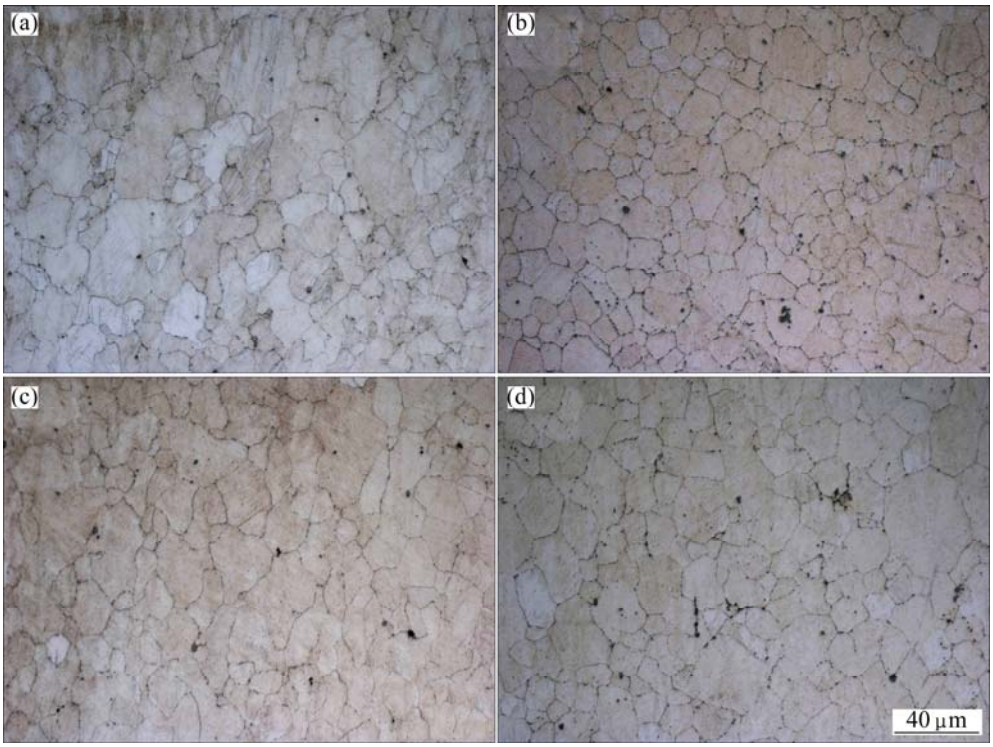

Fig. 7 Optical microstructures of ZA61 Mg alloy with compression strain of 60% at 350 °C (a, b) and 400 °C (c, d) with different strain rates: (a) 350 °C, 0.01 s^{-1}; (b) 350 °C, 1 s^{-1}; (c) 400 °C, 0.01 s^{-1}; (d) 400 °C, 1 s^{-1}

with the increase of strain rate at a fixed temperature. Deformation temperature has an important effect on the extent of recrystallization. At high temperatures of 350 °C and 400 °C, the dislocations are more prone to move and recombine, which helps the occurrence of completely dynamic recrystallization. The recrystallized grain size may be related to the work-hardening rate [18]. There is higher dislocation density with the increase of strain rate at a fixed temperature, which provides more nucleuses for dynamic recrystallization, and work hardening occurs in the newly formed recrystallized grains. The size becomes limited as the driving force for the further growth is reduced. The growth of the new grains is also limited with the increasing strain rate, thereby the size of dynamically recrystallized grains decreases with the increase of strain rate; when deformed at 350 °C with the strain rate of 1 s^{-1}, the grain size is the least.

3.4 Co-effects of strain rate and deformation temperature

The processing maps of the ZA61 magnesium alloy at different true strains are shown in Fig. 8. The strain of 0.1 is considered to represent strains close to the critical strain for most of the strain rates, the strain of 0.6 corresponds to the strain rates at the steady state conditions. The contours represent the efficiency of power dissipation, which characterizes the rate of microstructure evolution during the hot deformation. The black areas stand for the flow instability with negative values. It can be found that there exists a significant effect of strain on the processing maps. When the ZA61 magnesium alloy deformed at the strain of 0.6 (steady state), the locations and areas of flow instability change and increase compared with the strain of 0.1, so it is important to confirm the suitable processing region especially for the hot deformation with large strains.

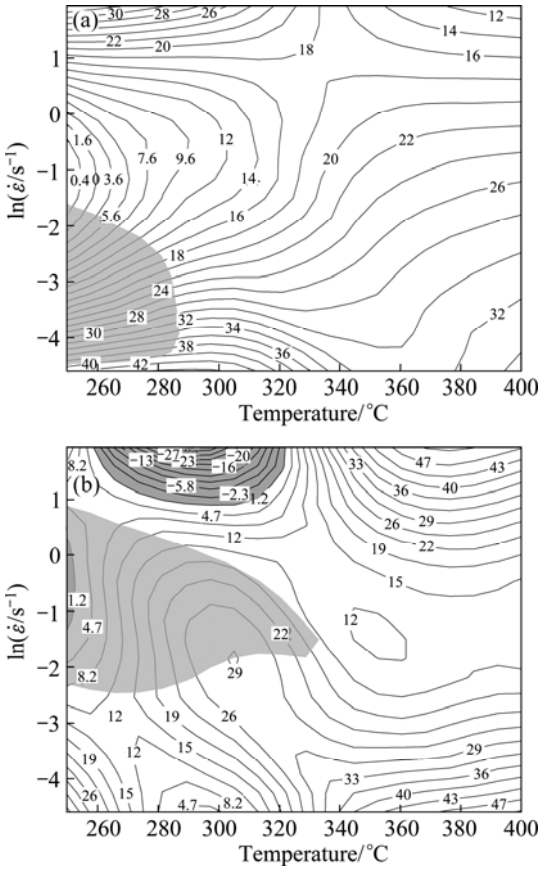

Fig. 8 Processing maps of ZA61 Mg alloy at different true strains: (a) ε=0.1; (b) ε=0.6

It was proved that the peak efficiency of dynamic recrystallization ranges from 30% to 40% for the materials with low stacking fault energies, such as magnesium alloys, and completely dynamic recrystallization is desirable during the deformation [19,20], so the suitable deformation conditions for the ZA61 magnesium alloy would be the areas with the peak efficiency ranging from 30% to 40%, meanwhile, not locate at the flow instability zone. There are two domains according with the demands at the strain of 0.6: 330−400 °C and 0.01−0.03 s^{-1}; 340−400 °C and 1.5−3 s^{-1}. The condition of 330−400 °C and 0.01−0.03 s^{-1} has been proved to be consistent with the microstructure observations from Fig. 5. Besides, another region was analyzed based on the microstructure observations with the strain rate of 3 s^{-1} at 350 °C, 400 °C as presented in Fig. 9. It can be found that there is no completely

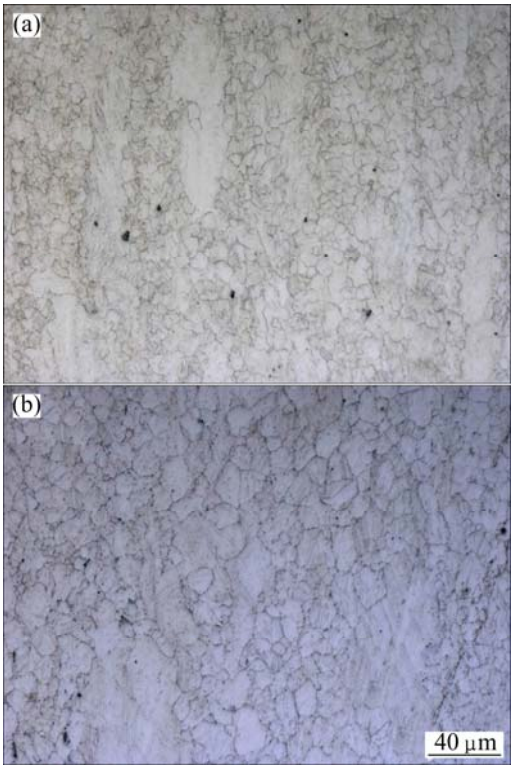

Fig. 9 Optical microstructures of ZA61 Mg alloy with compression strain of 60% and strain rate of 3 s^{-1} at 350 °C (a) and 400 °C (b)

dynamic recrystallization, so the scopes of 330−400 °C and 0.01−0.03 s^{-1} are considered a suitable deformation region. Besides, finer recrystallized grain size means better properties of ZA61 magnesium alloy after deformation, so it should be taken into account. According to the microstructure analysis before, when deformed at 350 °C with the strain rate of 1 s^{-1}, the size of completely dynamically recrystallized grains is the least, although the efficiency of power dissipation is only 22%. Therefore, the suitable deformation condition is concluded to be the domains of 330−400 °C and 0.01−0.03 s^{-1} and 350 °C and 1 s^{-1} combined with the deformation microstructure observation and the hot processing maps.

4 Conclusions

1) The hot deformation behavior of ZA61 magnesium alloy significantly depends on the deformation temperature and strain rate.

2) The activation energy (Q) and the stress exponent (n) are calculated to be 166 kJ/mol and 5.99, respectively. The flow rule of ZA61 could be expressed by the hyperbolic sine-type equation as

$$\dot{\varepsilon} = 3.16\times10^{13}\left[\sinh(0.010\sigma)\right]^{5.99}\exp[-1.66\times10^{5}/(RT)]$$

3) Incompletely dynamically recrystallized grains can be found at grain boundaries and twins with the strain rates ranging from 0.01 to 1 s^{-1} at 250 °C. At 350−400 °C, the microstructure is completely dynamically recrystallized and the grain size decreases with the increasing strain rate.

4) The suitable deformation conditions are confirmed to be 330−400 °C and 0.01−0.03 s^{-1}, and 350 °C and 1 s^{-1}.

References

[1] AGHION E, BRONFIN B. Magnesium alloys development towards the 21st century [J]. Materials Science Forum, 2000, 350−351(1): 19−28.

[2] YANG Y Q, LI B C, ZHANG Z M. Flow stress of wrought magnesium alloys during hot compression deformation at medium and high temperatures [J]. Materials Science and Engineering A, 2009, 499(2): 238−241.

[3] YU Kun, LI Wen-xian, WANG Ri-chu, MA Zheng-qing. Researches, developments and applications of wrought magnesium alloys [J]. The Chinese Journal of Nonferrous Metals, 2003, 13(2): 277−288. (in Chinese)

[4] WANG Ya-xiao, ZHOU Ji-xie, WANG Jie, LUO Tian-jiao, YANG Yuan-sheng. Effect of Bi addition on microstructures and mechanical properties of AZ80 magnesium alloy [J]. Transactions of Nonferrous Metals Society of China, 2011, 21(4): 711−716.

[5] ZHANG Ding-fei, SHI Guo-liang, DAI Qing-wei, YUAN Wei, DUAN Hong-ling. Microstructures and mechanical properties of high strength Mg−Zn−Mn alloy [J]. Transactions of Nonferrous Metals Society of China, 2008, 18(1): 59−63.

[6] ZHANG Z, COUTURE A. An investigation on the properties of Mg−Zn−Al alloy [J]. Scripta Mater, 1998, 39(1): 45−53.

[7] HONO K, MENDIS C L, SASAKI T T, OH-ISHI K. Towards the development of heat-treatable high-strength wrought Mg alloys [J]. Scripta Mater, 2010, 63(4): 710−715.

[8] CHEN Xiao-qiang, LIU Jiang-wen, LUO Cheng-ping. Research status and development trend of Mg−Zn alloys with high strength [J]. Materials Review, 2008, 22(1): 58−62. (in Chinese)

[9] CHEN Zhen-hua. Magnesium alloys [M]. Beijing: Chemical Industry Press, 2004. (in Chinese)

[10] PARK S S, BAE G T, KANG D H, JUNG I H, SHIN K S, KIM N J. Microstructure and tensile properties of twin-roll cast Mg–Zn–Mn–Al alloys [J]. Scripta Mater, 2007, 57(4): 793−796.

[11] OH-ISHI K, HONO K, SHIN K S. Effect of pre-aging and Al addition on age-hardening and microstructure in Mg−6wt%Zn alloys [J]. Materials Science and Engineering A, 2008, 496(3): 425−433.

[12] SAKAI T, JONAS J J. Dynamic recrystallization–mechanical and microstructural considerations [J]. Acta Metallurgica, 1984, 32(2): 189−209.

[13] SELLARS C, MCTEGART W J. On mechanism of hot deformation [J]. Acta Metallurgica, 1966, 14(6): 1136−1138.

[14] MCQUEEN H J, RYAN N D. Constitutive analysis in hot working [J]. Materials Science and Engineering A, 2002, 322(1): 43−63.

[15] SOMEKAWA H, HIRAI K, WATANABE H, TAKIGAWA Y, HIGASHI K. Dislocation creep behavior in Mg–Al–Zn alloys [J]. Materials Science and Engineering A, 2005, 407(1): 53−61.

[16] WU Hong-yu, YANG Jie-chen, LIAO Jing-hao, ZHU Feng-jun. Dynamic behavior of extruded AZ61 Mg alloy during hot compression [J]. Materials Science and Engineering A, 2012, 535(1): 68−75.

[17] YIN D L, ZHANG K F, WANG G F, HAN W B. Warm deformation behavior of hot-rolled AZ31 Mg alloy [J]. Materials Science and Engineering A, 2007, 392(3): 320−325.

[18] FATEMI-VARZANEH S M, ZAREI-HANZAKI A, BELADI H. Dynamic recrystallization in AZ31 magnesium alloy [J]. Materials Science and Engineering A, 2007, 456(1): 52−57.

[19] MWEMBELA A, KONOPLEVA E, MCQUEEN H J. Hot workability of Mg alloys AZ31 and AZ31−Mn [J]. Recent Developments in Light Metal, 1994(3): 365−373.

[20] WANG C Y, WANG X J, CHANG H, WU K, ZHENG M Y. Processing maps for hot working of ZK60 magnesium alloy [J]. Materials Science and Engineering A, 2007, 464(1): 52−58.

Mg−6Zn−1Al−0.3Mn 镁合金的热压缩变形行为及变形组织

史宝良，罗天骄，王 晶，杨院生

中国科学院 金属研究所，沈阳 110016

摘 要：采用 Gleeble 热模拟方法研究 Mg−6Zn−1Al−0.3Mn 变形镁合金在温度为 200~400 °C，应变速率为 0.01~7 s^{-1} 条件下的热压缩变形行为。结果表明，变形温度和应变速率显著影响其热变形行为。通过计算获得了热变形激活能及应力指数分别为 Q=166 kJ/mol，n=5.99，且其本构方程为 $\dot{\varepsilon}=3.16\times10^{13}[\sinh(0.010\sigma)]^{5.99}\exp[-1.66\times10^5/(RT)]$。热压缩显微组织观察表明：在应变速率为 0.01~1 s^{-1} 的条件下，在 250 °C 热压缩变形时初始晶粒晶界及孪晶处发生了部分动态再结晶，而在高温(350~400 °C)条件下，发生了完全动态再结晶且再结晶晶粒尺寸随着应变速率的增加而减小。获得的较优的变形条件为温度 330~400 °C、应变速率为 0.01~0.03 s^{-1} 以及 350 °C、应变速率为 1 s^{-1}。

关键词：变形镁合金；热压缩；应力；应变；再结晶

(Edited by Xiang-qun LI)